Biochimica et Biophysica Acta, 382 (1975) 542–551

BBA 76899

RAMAN AND RESONANCE-RAMAN SCATTERING BY ERYTHROCYTE GHOSTS

DONALD F. H. WALLACH and SURENDRA P. VERMA

Division of Radiobiology, Tufts-New England Medical Center, 136 Harrison Avenue, Boston, Mass. 02111 (U.S.A.)

(Received September 4th, 1974)
(Revised manuscript received October 21st, 1974)

SUMMARY

1. We present the laser-Raman spectra of human erythrocyte ghosts, isolated by standard conditions and compare these with the spectra of lecithin liposomes and fat-free serum albumin.

2. The hydrocarbon stretching modes of membrane lipids are temperature sensitive and may serve as an index of hydrocarbon chain motion.

3. The Amide I and Amide III bands of ghosts in H_2O and ^2H_2O, indicate a mixture of α-helical and unordered conformation, but do not allow a quantitative estimate of secondary structure.

4. Strong, scattering bands at 1530 and 1165 cm^{-1} are attributable to conjugated double bond systems, probably of membrane-associated carotenoids. Their high intensity is due to resonance enhancement.

INTRODUCTION

Spectroscopic methods can provide important information about the structures of model and biological membranes. As detailed in a recent review [1] two types of strategy have been employed. Of these, the probe approach relies on signals from fluorescent or paramagnetic reporter groups artificially introduced into the membranes. These can provide information on the polarities, viscosities and other properties of their immediate environments. However, they may also act as perturbants [1, 2].

The second strategy utilizes signals derived from membrane components themselves. The techniques in this category include measurements of optical activity, nuclear magnetic resonance, intrinsic protein fluorescence, infrared absorption and Raman scattering [1]. Each technique has its shortcomings [1] and Raman spectroscopy is still in its infancy as far as membrane applications are concerned. This method has, however, already been applied to structural investigations of artificial lipid membranes [3–5]. In addition, resonance-enhanced Raman spectra have been obtained from the membranes of *Halobacterium halobium* [6] and from retinal rod outer seg-

ments [7]. A preliminary report on the Raman spectrum of erythrocyte ghosts has also been published [8], but does not provide significant detail.

Raman spectra can yield a wealth of information, since any bond motion which involves a polarizability change may produce a Raman line. This is apparent from model studies on polypeptides [9–11], model lipid systems [3–5, 12], as well as investigations of pure proteins [13–15]. These investigations suggest that Raman spectroscopy can provide information about the state of membrane lipids, the conformation of membrane proteins and the nature of lipid protein interactions.

In this report we describe the Raman spectra of erythrocyte ghosts in the range of 700–3100 cm^{-1}, and correlate the spectral characteristics of the membranes with those of selected lipid and protein models.

EXPERIMENTAL

Materials

Fat-free bovine serum albumin (Sigma, St. Louis, Mo.) was examined as a solution of 25 mg/ml. Liposomes were prepared from egg yolk phosphatidylcholine (Lipid Products, South Nutfield) by suspending 10 mg of the lipid in 1 ml of 5 mM phosphate (pH 7.4) and sonicating for 10 min at 20 °C (Sonic Dismembranator, Quigley-Rochester, Rochester, N.Y.; power step 30).

Erythrocyte ghosts were prepared from freshly drawn, heparinized blood as in ref. 16, resuspended in 5 mM phosphate, pH 7.4, and pelleted at $6 \cdot 10^6$ $g_{av} \cdot$ min, using a Spinco ultra centrifuge (L265B, Rotor SW56). Protein concentration was determined fluorometrically as in ref. 16.

Spectroscopy

Spectra were recorded with a Ramalog 4 Raman Spectrometer (Spex Industries, Metuchen, N.J.) interfaced to an Interdata (Model 70) Computer. Unless stated otherwise, we used 100 mW power at 488 nm from an Argon-ion laser (Spectra Physics Model 164). However, in some experiments we tuned the laser at 427.2, 488.0, 496.5, 501.7 or 514.5 nm. Scanning was in steps of 1 cm^{-1}. Photon detection was by an RCA C31034 photomultiplier, cooled thermoelectrically to −30 °C and Raman scattering was recorded in terms of photons/s. The maximum dwell time for each frequency step was 1 s. The "dark" count was <100 counts/s and the "light" counts ranged from $1 \cdot 10^4$–$2 \cdot 10^4$ counts/s to $3 \cdot 10^4$–$4 \cdot 10^4$ counts/s. The time required to obtain reliable spectra (700 to 3100 cm^{-1}) was 20–26 min. The photon counts were stored in the computer memory during scanning. In general, scans were repeated 2–3 times. The stored spectra were then plotted on the Ramalog recorder after adjustment of plotting parameters (scale).

Liposome suspensions, albumin solutions, ghost pellets were transferred to 0.9 mm ID Kimex capillaries and these placed in a Harney-Miller cell [17] for temperature control. Temperature was regulated by a flow of nitrogen and controlled by a telethermometer to ± 2 °C as determined by melting point determinations on reference lipids. Unless stated otherwise the spectra were recorded at 20 °C. Less than 10 μg albumin or erythrocyte ghost protein was exposed to the laser beam; the value for liposomes was about 4 μg phospholipid.

RESULTS AND DISCUSSION

A typical Raman spectrum of erythrocyte membranes is represented in Fig. 1. The spectrum presented is a computer-averaged plot of three scans. Our spectral assignments (Table I) are based on reported Raman spectra of different lipids and proteins.

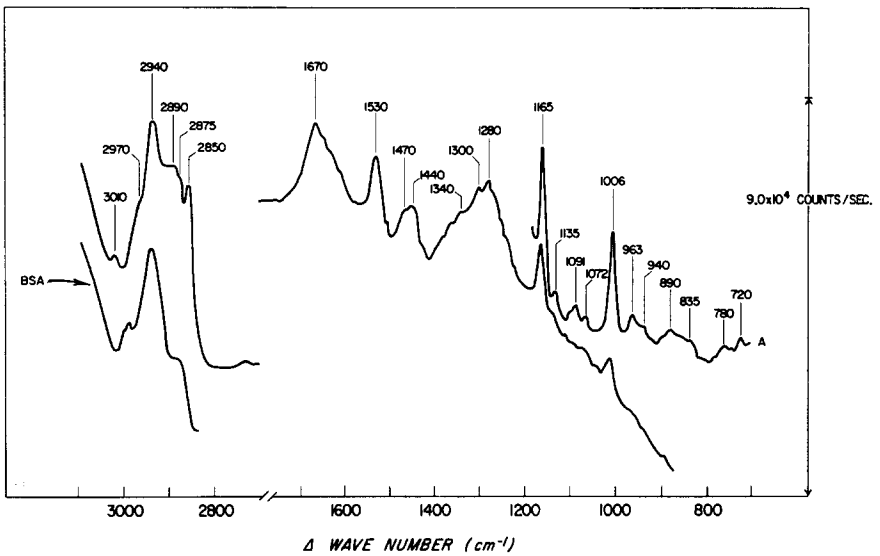

Fig. 1. Raman spectrum of erythrocyte ghosts in 0.005 M phosphate, pH 7.4. Ordinate presents scattering intensity in photons/s. Full scale = $9 \cdot 10^4$ photons/s. Abscissa presents difference of frequency from laser frequency in Δcm^{-1}. Plotting steps: 50 cm^{-1}/s. Excitation at 488.0 nm (20 492 cm^{-1}); Slits, 8 cm^{-1}; power 100 mW; Temperature, 20 °C. Curve A represents a scale expansion ($6.0 \cdot 10^4$ photons/s full scale) of the 700–1180-cm^{-1} region and was recorded without cutoff filter. Curve BSA represents the spectrum of bovine serum albumin in the 2800–3100 cm^{-1} region (full scale, $9 \cdot 10^4$ photons/s).

Hydrocarbon stretching modes

Ghosts exhibit hydrocarbon stretching modes in the 2800–3000 cm^{-1} region. Prominent, sharp bands occur at 2850 and 2940 cm^{-1}. There is also a broad band at 2890 cm^{-1} and a shoulder at 2970 cm^{-1}. These bands represent contributions from both the protein and lipid components of the membranes.

The sharp bands at 2850 and 2940 cm^{-1} arise from symmetric and antisymmetric CH_2 stretching, respectively. Thy symmetric CH_2-stretching band of fat-free serum albumin is rather weak and lies at 2875 cm^{-1} (Fig. 1), whereas liposomes exhibit a strong sharp band at 2850 cm^{-1} (Fig. 2, ref. 4). We conclude, therefore, that the 2850-cm^{-1} band of ghosts arises predominantly from membrane lipids.

The antisymmetric CH_2-stretching band of fat-free albumin is very strong, but liposomes show only a shoulder at this frequency. We therefore suggest that the strong 2940-cm^{-1} band of erythrocyte membranes contains a greater contribution from membrane proteins than from membrane lipids.

Liposomes exhibit a sharp band at 2890 cm^{-1}. This includes contributions

TABLE I

RAMAN FREQUENCIES AND INTENSITIES OF ERYTHROCYTE GHOSTS, EGG LECITHIN AND BOVINE SERUM ALBUMIN

Relative intensities are given in brackets. The 1006-cm^{-1} band (10) is taken as an internal reference (erythrocyte ghost and bovine serum albumin). ν = stretching; sh = shoulder; def. = deformation; sym. = symmetric; antisym. = antisymmetric; asym. = asymmetric.

Frequency			Tentative assignment
Ghost	Bovine serum albumin	Egg lecithin	
720 (1.4)		720	Choline
780 (1.3)			
835 (2)	830 (2.5)	—	Tyr
	860 (2.5)	—	
890 (2)	900 (1.5)	—	
940 (2)	950 (4)	—	
960 (3)			ν (C–C)
970 (2.3)			Amide III (^2H_2O)
1006 (10)	1005 (10)	—	Trp, Phe
	1030 (3.3)		
1072 (1.4)		1065	
			ν (C–N)+ν(C–C)
1091 (2.4)		1095	
1135 (3)	1130 (2.5)	1128	
1165 (16)			ν (=C–C=)
	1180 (2.5)		
	1210 (2.5)		Tyr
1280 (26)	1250 (6)		Amide III
1300 (24)		1298	CH_2 wag
1340 (sh)	1348 (7.5)		Trp and CH def.
	1410 Sh		—
1440-1470 (12)	1450 (10)	1440, 1460	CH_2 scissoring
	1470 (8)		
1530 (20)	1550 (2.5)	—	(–C=C–); Trp
1640 (18)	1610 (sh)	1655	Amide I, H_2O
1670 (20)	1635 (sh)		
	1660		
		1735	Carboxyl
2730		2720	—
2850		2850	ν sym. CH_2
	2875		
2890		2890	ν sym. (CH_3+CH_2)
2940	2940	2930 (sh)	ν antisym. (CH_2)
2970	2965 (sh)	2960 (sh)	ν asym. (CH_2)
3010		3012 (sh)	

from antisymmetric CH_3 stretching and symmetric CH_2 stretching. Albumin does not exhibit a band in this region. Accordingly, the moderately broad 2890-cm^{-1} band in ghosts presumably represents a contribution of membrane lipids.

Brown et al. [4] report that, in the cases of dipalmitoylphosphatidylcholine and dipalmitoylphosphatidylethanolamine, the intensity ratio 2890 cm^{-1} : 2850 cm^{-1} decreases with increasing temperature. Since the hydrocarbon chain motion of

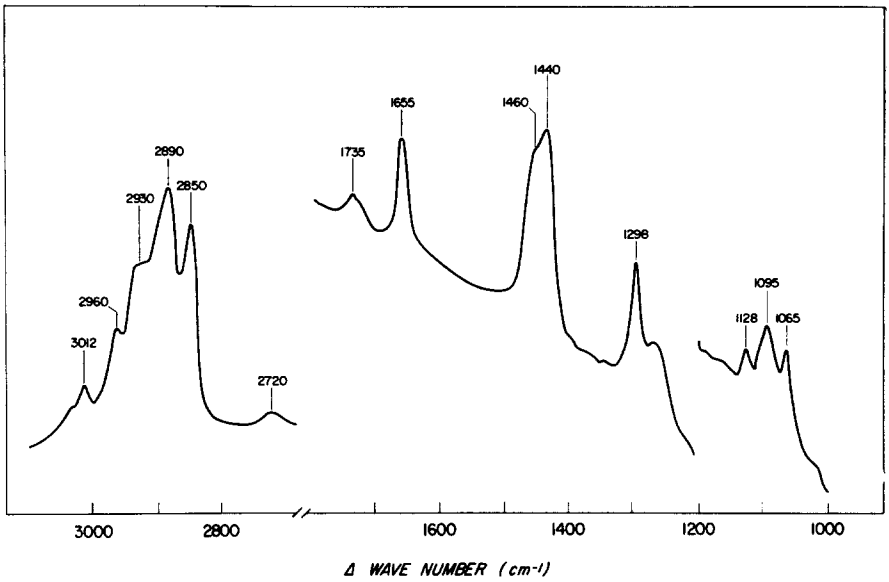

Fig. 2. Raman spectrum of egg lecithin liposomes. Ordinate full scale, $3 \cdot 10^4$ photons/s. Plotting steps, 40 cm^{-1}/s. Excitation at 488.0 nm; slits, 8 cm^{-1}; power, 100 mW; temperature, 20 °C.

phospholipids is known to increase with temperature, these authors suggest that the 2890 cm^{-1} : 2850 cm^{-1} can serve as an index of acyl chain mobility. Our data on egg lecithin are in general agreement with this conclusion. However, this ratio cannot necessarily be transferred to other systems, for example erythrocyte ghosts. These membranes do not exhibit a significant change in the relative intensities at 2890 and 2850 cm^{-1} over a 20 °C temperature range. This may be because the 2890-cm^{-1} band of the lipids is mixed with the 2875-cm^{-1} contribution of the proteins to yield rather diffuse scattering between 2875 and 2890 cm^{-1}. In contrast, the intensity ratio 2940 cm^{-1} : 2850 cm^{-1} of the erythrocyte membranes does vary with temperature. It is 1.1 at 20 °C and 1.3 at 7 °C. However, the 2940-cm^{-1} band of albumin does not change with temperature relative to other scattering peaks. Since proteins do not appear to contribute significantly to Raman scattering at 2850 cm^{-1}, we accordingly suggest that the lesser 2940 cm^{-1} : 2850 cm^{-1} ratio of ghosts at 20 °C compared to 7 °C reflects a greater acyl chain mobility at the higher temperature.

Amide I and Amide III regions

The Amide I band of ghosts in aqueous suspension is difficult to assign due to the strong Raman scattering of water in this region. We observe a peak at 1670 cm^{-1} atop the water band and a shoulder at 1645 cm^{-1} attributed to the water (Fig. 1). In the case of poly-L-lysine one observes a strong band at 1670 cm^{-1} when the polymer is in the antiparallel β-conformation [9, 10]. However, "unordered" poly-L-lysine yields strong bands at 1653, 1665 and 1683 cm^{-1} [9], while the α-helical conformation exhibits a strong, scattering peak at 1647 cm^{-1} [9]. If the peak at 1670 cm^{-1} were due to anti-parallel β-structuring, one should see a strong peak at 1631 cm^{-1} [9]. We do not observe this. Moreover, infrared spectra of lyophilized erythrocyte

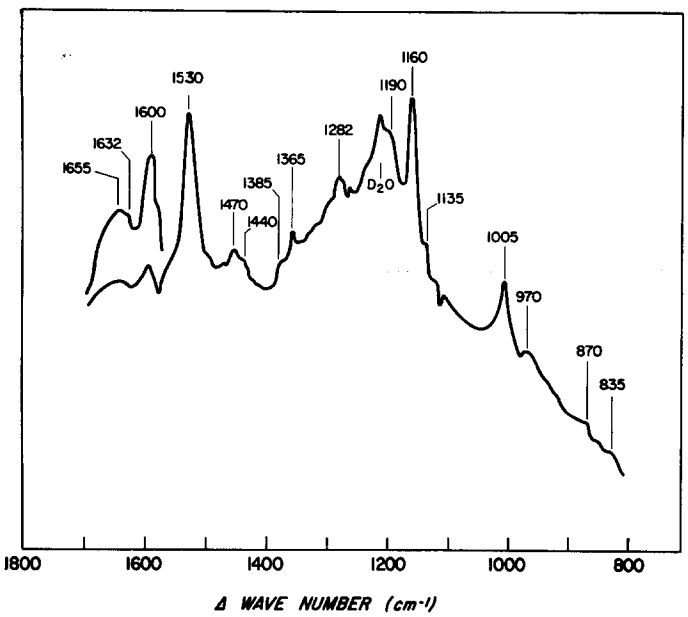

Fig. 3. Raman spectrum of erythrocyte ghosts in ^2H_2O (0.005 M phosphate pH 8.0). Ordinate full scale, $9 \cdot 10^4$ photons/s. Plotting steps, 50 cm^{-1}/s. Excitation at 488.0 nm; slits, 8 cm^{-1}; power, 100 mW; temperature, 20 °C.

ghosts [18] give no evidence of β-structure, except during ATP hydrolysis, which does not apply here. We tentatively suggest that the 1670-cm^{-1} band is a contribution of peptide in "unordered" array.

After equilibrating the ghosts in 99.9% ^2H_2O at 4 °C for 12 h, the water band at 1645 cm^{-1} is eliminated (Fig. 3). We now observe two peaks in the Amide I region, one at 1655 and one at 1632 cm^{-1}. Poly-L-lysine in ^2H_2O yields scattering bands at 1658 cm^{-1} in the β-structure, and at 1660 cm^{-1} in the "unordered" conformation [10]. One can therefore not distinguish between these conformations on the basis of scattering near 1660 cm^{-1}. However, the shoulder near 1632 cm^{-1} in ^2H_2O is consistent with α-helix [10]. It should be noted that infrared evidence indicates that substitution of ^2H_2O for H_2O actually induces a transition to a β-structure [18].

The sharp peak which appears at 1600 cm^{-1} after deuteration is tentatively assigned to tyrosine and/or phenylalanine. It presumably emerges as result of elimination of the water background.

In aqueous ghost suspensions the Amide III band appears at 1280 cm^{-1}, but overlaps with the 1300 cm^{-1} band due to CH_2 twisting. The resulting doublet does not allow exact frequency assignments. In α-helical poly-L-lysine the Amide III band is weak and lies near 1240 cm^{-1} [10]. In contrast, the Amide III band at 1240 cm^{-1} is very strong in β-structured poly-L-lysine [10]. In unordered poly-L-lysine the Amide III band lies at 1243 cm^{-1}. Ghost suspensions in ^2H_2O reveal a small band at 970 cm^{-1}. This might represent the Amide III vibration which is shifted downfield upon deuteration. In the case of ^2H_2O solutions of poly-L-lysine, the Amide III band is reported to lie at 982, 987 and 983 cm^{-1} for the α-helical, β- and "unordered"

conformations respectively [10]. However, precise assignments are complicated by the C-C and C-N stretching vibrations which occur near 1000 cm^{-1}.

To sum, the Amide I and Amide III regions, although conformationally sensitive, do not allow conformational analyses of ghost proteins by direct spectroscopy. This may be possible however, by difference spectroscopy.

1530- and 1165-cm^{-1} bands

Erythrocyte membranes exhibit strong Raman scattering bands at 1530 and 1165 cm^{-1}. We have evaluated these peaks using the 1006-cm^{-1} tryptophan band as internal reference, since this peak does not vary in intensity or position with the frequency of the exciting light. The relative intensities of both the 1530-cm^{-1} band and the 1165-cm^{-1} peak increase as the exciting wavelength is decreased (Fig. 4). In addition, both bands decrease in intensity with time of irradiation (up to 80 %); this effect is more pronounced at shorter excitation wavelengths (488.0 nm, 427.2 nm). Both bands sharpen and intensify (up to 40 %) upon temperature reduction to −10 °C. The bands also intensify when the pH is lowered from 7.4 to 5.0, upon addition of lysolecithin and after trypsinization. In contrast, the intensities (with respect to 1006 cm^{-1}) of both bands drops to 44 % upon addition of sodium dodecylsulfate (to a concentration of 100 μg/ml). The bands are almost abolished by heating at 60 °C for 20 min. These Raman bands are observed in the lipid extracted from ghosts with chloroform/methanol (2 : 1, v/v). Moreover, the material responsible can be further extracted into either diethyl ether or hexane: these do dissolve membrane phosphatides.

These data indicate that both bands represent double and single bond stretching modes, respectively, of conjugated unsaturated chains, enhanced by vibronic coupling to electronic absorption. We assign these bands to membrane carotenoids, which exhibit resonance Raman scattering at frequencies very close to what we observe, e.g. 1527 and 1158 cm^{-1} for β-carotene [19]. Our contention is supported by the fact that hexane extracts yield fluorescence spectra characteristic of conjugated polyenes and by the effects of prolonged irradiation and high temperature.

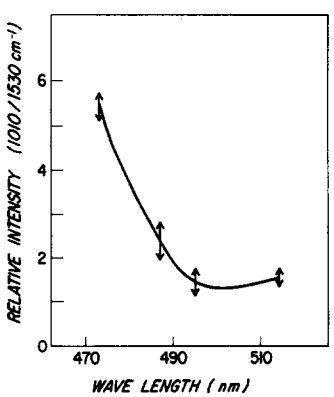

Fig. 4. Intensity of 1530-cm^{-1} band of erythrocyte ghosts relative to that of the 1006-cm^{-1} band as a function of exciting wavelength. Slits, 8 cm^{-1}; temperature, 20 °C.

CH_3-CH_2 deformation

These frequencies lie between 1440 and 1470 cm^{-1} in both ghosts and in egg lecithin liposomes. In the case of the phosphatide dispersion we can resolve two bands at 1440 and 1460 cm^{-1} at 20 °C. When the liposomes are heated to 60 °C, these bands merge and a single component appears at 1455 cm^{-1}; this single band reflects the liquid state of the acyl chains. In liposomes, therefore, the position and sharpness of deformation bands thus serve as an index of hydrocarbon chain mobility. In ghosts interpretation of this region is complicated by the diffuse contribution by proteins [13].

Other vibrations

Ghosts exhibit prominent Raman scattering peaks at 1135, 1091 and 1072 cm^{-1}. Previous publications on the Raman spectra of diverse lipids [3, 5, 12] have assigned these bands to the C–C stretching modes of acyl chains. Moreover, the intensity of the 1065-cm^{-1} band of phosphatides relative to that of the 1135-cm^{-1} band has been proposed as measure of acyl chain mobility [3, 5, 8]. However, C–N stretching vibrations arising from the amino acid residues also occur in this region [10, 13]. Since ghosts constitute a mixture of lipid and proteins, it becomes hard to specify the source of these bands. Accordingly, we feel that the intensity of the 1072-cm^{-1} band of ghosts (1065 cm^{-1} in egg lecithin) relative to that of the 1135 cm^{-1} band cannot give a reliable index of lipid hydrocarbon chain mobility.

The bands at 963 and 940 cm^{-1} in ghost can be assigned to C–C stretching. Bovine serum albumin also exhibits peaks in this region [13] but they are not found in diverse pure lipids. We therefore suspect that these bands originate from membrane proteins.

The C–N stretching modes of substances such as $(CH_3)_2NH_2^+$, $(CH_3)_3NH^+$, $(CH_3)_4N^+$ appear at 895, 821 and 752 cm^{-1} respectively [20], i.e. their frequency depends upon the substitution on the nitrogen atom. The 720-cm^{-1} band in egg lecithin might thus be attributed to the choline moiety [4]. Accordingly we tentatively assign the 720-cm^{-1} band of ghosts to the choline head group of the membrane lecithin.

Heat denaturation

Ghosts denatured by heating at 60–70 °C for 15 min exhibit a high fluorescence background when excited at 488 nm. However, good spectra can be recorded at 514.5 nm, where we observe the following: (a) The Amide I band sitting on top of the water band at 1670 cm^{-1}, shifts to 1655 cm^{-1} with appearance of another band at 1600 cm^{-1}. (b) The intensity of the 1530 cm^{-1} band is markedly diminished. (c) The intensity ratio 2940 cm^{-1} : 2850 cm^{-1} shifts to 1.5.

Effect of pH

We lowered the pH of erythrocyte ghost to 5.5. At pH 5.5 we find the following: (a) The Amide I band (mixed with H_2O band) is shifted to 1655 cm^{-1}; (b) the ratio of 1530 cm^{-1} : 1006 cm^{-1} is 3.0 compared to 2.5 at pH 7.4, i.e. the 1530-cm^{-1} band has increased in intensity; (c) the Amide III band remains at 1280 cm^{-1}. The intensity ratio of 2940 cm^{-1} : 2850 cm^{-1} remains at 1.1.

GENERAL COMMENTS

We demonstrate that one can obtain well resolved Raman spectra (700–3100 cm^{-1}) from erythrocyte ghosts prepared by standard techniques. Many scattering bands arise from both membrane lipids and membrane proteins, but other spectral components are dominated by only one of the two major membrane constituents.

Thus membrane proteins contribute uniquely in the region between 1630 and 1670 cm^{-1} (Amide I), 1200 to 1280 cm^{-1} (Amide III) about 1600 cm^{-1} (tyrosine), approx. 1006 cm^{-1} (aromatic amino acids), approx. 890 (tryptophan), and approx. 835 (tyrosine). Moreover, the sharp band observed in ghosts at 2940 cm^{-1} can be considered to arise primarily from membrane proteins. We cannot now state how useful these bands will be in the analysis of membrane protein architecture.

The contributions of membrane lipids are 2-fold. (a) Simple Raman scattering attributable predominantly to phosphatide acyl chains occurs in the hydrocarbon stretching region and the hydrocarbon deformation region. The former is temperature sensitive and may serve to analyze an acyl chain mobility. This could prove useful in evaluating lipid-protein interactions. (b) Our most unique finding perhaps is the demonstration of resonance Raman bands at 1530 and 1165 cm^{-1}. These are attributable to conjugated polyene systems in membrane lipids, most likely carotenoids. These represent important but trace components of erythrocyte membranes and their detection depends entirely on the strong resonance enhancement of Raman scattering in regions of electronic excitation. This has been well documented by Rimai et al. [19], who show that maximum resonance enhancement of the 1527- and 1158-cm^{-1} bands of β-carotene occurs upon excitation at 476 nm. The degree of enhancement is remarkable and allows observation of the 1527- and 1158-cm^{-1} lines at concentrations of 10^{-7} M [19]. This corresponds to $5.4 \cdot 10^{-5}$ mg/ml. Our membrane samples were studied at a concentration of 20 mg protein per ml, i.e. about 8 mg total lipid per ml. Accordingly, the carotenoid scattering lines could arise from as little as $7 \cdot 10^{-4}$ % of the membrane lipid.

Retinol, another carotenoid, has been suggested as a fluorescent probe for membrane lipids [21]. We find that the intensities of the carotenoid bands can be influenced by manipulations which alter the state of membrane lipids (cooling; lysolecithin) as well as procedures which primarily alter the state of membrane proteins (trypsinization; change of pH) [22]. These data suggest that conjugated polyenes may serve as sensitive "Raman-active" membrane probes. We will treat this topic in a subsequent communication.

ACKNOWLEDGEMENT

Supported by grants No. CA-13061 and GB-32123 from the U.S. Public Health Service and the National Science Foundation, respectively, and award PRA-74 from the American Cancer Society (D.F.H.W.).

REFERENCES

1 Wallach, D. F. H. and Winzler, R. (1974) Evolving Strategies and Tactics in Membrane Research, Chapters 3–8, Springer-Verlag, New York
2 Keith, A. D., Sharnoff, M. and Cohn, G. E. (1973) Biochim. Biophys. Acta 300, 379–419

3 Lippert, J. L. and Peticolas, W. L. (1971) Proc. Natl. Acad. Sci. U.S. 68, 1572–1576
4 Brown, K. G., Peticolas, W. L. and Brown, E. (1973) Biochem. Biophys. Res. Commun. 54, 358–364
5 Mendelsohn, R. (1972) Biochim. Biophys. Acta 290, 15–21
6 Mendelsohn, R. (1973) Nature 243, 22–24
7 Rimai, L., Kilponen, R. G. and Gill, D. (1970) Biochem. Biophys. Res. Commun. 41, 492–497
8 Bulkin, B. J. (1972) Biochim. Biophys. Acta 274, 649–651
9 Wallach, D. F. H., Graham, J. M. and Oseroff, A. R. (1970) FEBS Lett. 7, 330–334
10 Yu, T. J., Lippert, J. L. and Peticolas, W. L. (1973) Biopolymers 12, 2161–2176
11 Franconi, B., Tomlinson, B., Nafie, L. A., Small, W., and Peticolas, W. L. (1969) J. Chem. Phys. 51, 3993–4005
12 Larsson, K. (1973) Chem. Phys. Lip. 10, 165–176
13 Bellocq, A. M., Lord, R. C. and Mendelsohn, R. (1972) Biochim. Biophys. Acta 257, 280–287
14 Koenig, J. L. (1972) J. Polymer. Sci. Part D, 59–117
15 Chen, M. C., Lord, R. C. and Mendelsohn, (1973), Biochim. Biophys. Acta 328, 252–260
16 Fairbanks, G., Steck, T. L. and Wallach, D. F. H. (1971) Biochemistry, 10, 2606–2616
17 Miller, F. A. and Harney, B. M. (1970) Appl. Spectrosc. 2, 291–292
18 Graham, J. M. and Wallach, D. F. H. (1971) Biochim. Biophys. Acta 241, 180–194
19 Rimai, L., Kilponen, R. G. and Gill, D. (1970) J. Am. Chem. Soc. 92, 3824–3825
20 Cohn, E. J. and Edsall, J. T. (1965) in Proteins Aminoacids and Peptides, Chapter 1, Hafner Publishing Company, New York
21 Radda, G. K. and Smith, D. S. (1970) FEBS Lett. 9, 287–289
22 Verma, S. P. and Wallach, D. F. H. (1975) Biochim. Biophys. Acta, 382, 73–82